

Photon antibunching in single CdSe/ZnS quantum dot fluorescence

B. Lounis^{a,b,*}, H.A. Bechtel^a, D. Gerion^c, P. Alivisatos^c, W.E. Moerner^a

^a Department of Chemistry, Stanford University, Stanford, CA 94305-5080, USA

^b CPMOH, Université Bordeaux I, 33405 Talence, France¹

^c Department of Chemistry, University of California at Berkeley, CA 94720, USA

Received 26 June 2000; in final form 5 September 2000

Abstract

We investigate the fluorescence intensity correlation function of a single CdSe quantum dot (QD) using a start–stop experiment. We observe strong photon antibunching, a signature of non-classical light emission, over a large range of intensities (0.1–100 kW/cm²). The lack of coincidence at zero time delay indicates a highly efficient Auger ionization process, which suppresses multi-photon emission in these colloidal QDs. Using careful analysis of the saturation behavior of the coincidence histograms, the absorption cross-section of a single QD has also been derived. © 2000 Elsevier Science B.V. All rights reserved.

Over the past decade, interest in low-dimensional, mesoscopic systems, such as quantum dots (QDs), has grown dramatically. These semiconductor QDs bridge the gap between single molecules and the bulk solid state, thereby offering the opportunity to study the evolution of bulk properties. Additionally, their size-dependent optical properties make them ideal candidates for tunable absorbers and emitters in applications ranging from nanoscale electronics [1–3] to biological fluorescent labeling [4,5].

Since its inception, single molecule spectroscopy (SMS) has altered our understanding of fluorescent systems by elucidating the photo-

physics of isolated species in the absence of ensemble averaging [6]. The study of QDs has already benefited from the advent of single-molecule techniques, including the discovery of spontaneous spectral shifts [7], ultra-narrow transitions [8] and fluorescence intermittence [9]. Recent studies on fluorescence intermittence in QDs have indicated a distribution of on/off-times that follows a simple power law over five orders of magnitude from milliseconds to hundreds of seconds [10]. This ‘blinking’ is attributed to an Auger ionization process, which is initiated by the creation of multiple excitons in the QD. The energy released from the recombination of one electron–hole (e–h) pair may be transferred to another e–h pair, causing an electron (hole) to be ejected to the surface. Photoionized QDs exhibit significantly shorter emission lifetimes and lower quantum yield [11]. The emission is then restored

* Corresponding address. Fax: +33-5-56-84-6970.

E-mail address: lounis@yak.cpmoh.u-bordeaux.fr (B. Lounis).

¹ Permanent address.

when the ejected carrier returns to neutralize the QD.

QDs are often referred to as ‘artificial atoms’ because many of their optical properties, such as ultra-narrow transitions, arise from discrete, atomic-like energy levels. In this Letter, we reinforce this analogy by demonstrating that the intensity correlation function of the fluorescence from a single QD exhibits antibunching, a quantum optical property observed in light emitted from individual quantum systems, such as single atoms [12] and single molecules [13,14]. Since a finite time is required to cycle an atom (molecule) between its ground and excited states, a single atom (molecule) can never emit two photons at once. QDs differ from atoms and molecules since the creation of multiple excitons is possible in QDs. Consequently, if two e–h pairs can radiatively recombine, the simultaneous emission of two photons from a QD is then possible. Thus, one would expect different regimes of photon statistics because the probability of multiple exciton creation depends on excitation intensity.

We use a standard coincidence (start–stop) setup to study the fluorescence correlation function of single QDs. Samples of ZnS-coated CdSe QDs (18 Å radius, 575 nm peak emission, quantum yield ~40%) are prepared by spin coating clean glass coverslips with a 10^{-9} M solution of QD in toluene followed by a 2% by weight PMMA solution. The excitation beam, the 488 nm line of an Ar⁺ laser, is focused on the sample by a 1.4 NA oil-immersion objective in an inverted confocal microscope. The emitted photons collected by the same objective are filtered from the scattered excitation light by a band pass filter (35 nm FWHM) and sent through a 50/50 beam splitter onto two (start and stop) single photon counting avalanche photodiodes. A short pass filter is inserted before one of the photodiodes to suppress cross-talk between the two detectors. In our setup, single QDs are detected with a signal to background ratio greater than 500 (at the highest powers the maximum signal rate is 500 kHz per detector while the background signal is less than 1 kHz). The signals from the detectors are sent to a time-to-amplitude converter (TAC) followed by a pulse-height analyzer to create a histogram $C(\tau)$ of the delays τ

between consecutive photons detected from a single fluorescing QD. A constant delay is introduced in the stop channel to investigate negative times. To maximize the number of collected photons contributing to the coincidence histogram, the excitation beam is switched off by an acousto-optic modulator during the TAC dead time ~ 7 μ s.

Fig. 1 is a typical histogram $C(\tau)$ obtained from a single fluorescing QD. The histogram is recorded with a 200 ns TAC time window and a bin width t_{bin} of 0.2 ns. The dip in coincidences around zero delay is an unambiguous signature of antibunching. The very small number of coincidences (~ 3) at $\tau = 0$ is only due to the background and our time resolution of ~ 0.8 ns which is limited by the jitter in the detectors and electronics. This strong antibunching is observed over a wide range of excitation intensities (0.1–100 kW/cm²), indicating that the simultaneous radiative recombination of two excitons is unlikely. Recent measurements show Auger ionization rates [15] ($\sim 1/20$ ps⁻¹) which are much larger than the fluorescence decay rates [16] ($\sim 1/20$ ns⁻¹); this may explain the suppression of multi-photon emission we observe. This behavior is in contrast to that expected for

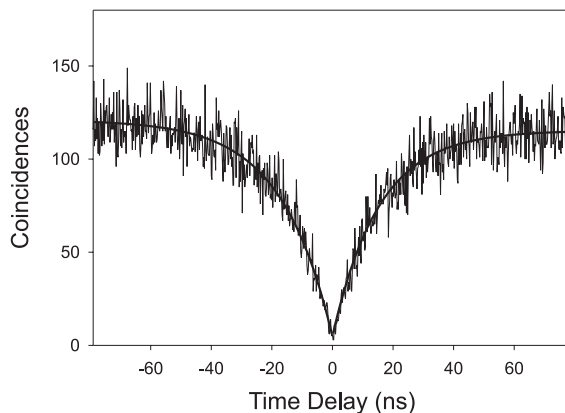


Fig. 1. Histogram of time delays between consecutive photon pairs (which is proportional to the intensity correlation function) detected from the fluorescence of a single CdSe QD. The time bin size is 0.2 ns, the excitation intensity is 11 kW/cm², and the accumulation time is 430 s. The histogram shows a dip that approaches zero (actual value ~ 3) at zero time delay, which is a clear signature of photon antibunching. The solid line represents a single exponential fit with a rise time constant of 16 (± 1) ns.

MBE-grown QDs, which may produce multiple photons under certain conditions [17].

To analyze the data, we review the precise meaning of the $C(\tau)$ measurement. The histogram $C(\tau)$ is proportional to the probability density $K(\tau)$ of detecting the *next* photon at time $t + \tau$ provided that there was a photon at time t

$$C(\tau) = T_{\text{acc}} t_{\text{bin}} R_1 K(\tau), \quad (1)$$

where T_{acc} is the accumulation time and R_1 is the count rate of the start detector. In contrast, the second-order intensity correlation function $G^{(2)}(\tau)$ is related to the probability density $J(\tau)$ of detecting a photon (not necessarily the next) at time $t + \tau$ provided that there was a photon at time t

$$G^{(2)}(\tau) = T_{\text{acc}} t_{\text{bin}} R_1 J(\tau). \quad (2)$$

However, as demonstrated by Reynaud [18], $K(\tau)$ is equivalent to $J(\tau)$ and consequently $C(\tau) = G^{(2)}(\tau)$ as long as τ is much smaller than the mean time between detected events. For a QD exhibiting an efficient Auger process, $J(\tau)$ is proportional to $p_1(\tau)$, the probability of finding the QD with one e–h pair, given that the QD had zero e–h pairs at $\tau = 0$ (i.e., $p_0(0) = 1$)

$$J(\tau) = \eta_2 \Phi_f T_1^{-1} p_1(\tau), \quad (3)$$

where η_2 is the detection efficiency of the stop channel, Φ_f the QD fluorescence quantum yield, and T_1 is the fluorescence lifetime, respectively.

To derive the expression $p_1(\tau)$, we consider the QD state-filling equations for cw excitation [19], including the off-state kinetics (blinking). Assuming that the QD is instantaneously ionized (and then becomes non-fluorescent) upon the creation of two excitons, we can write

$$\begin{aligned} \dot{p}_0 &= -W_1 p_0 + \frac{p_1}{T_1}, \\ \dot{p}_1 &= W_1 p_0 - \left(W_2 + \frac{1}{T_1} \right) p_1 + \frac{p_+}{\tau_{\text{off}}}, \\ \dot{p}_+ &= W_2 p_1 - \frac{p_+}{\tau_{\text{off}}}, \end{aligned} \quad (4)$$

where $p_{0,1}$ is the probability of finding the QD with 0 or 1 electron hole pairs, respectively, p_+ the probability of finding it ionized, τ_{off} the average lifetime for a trapped electron (hole) to return to the QD, and $W_{1,2} = \sigma_{1,2} I \lambda / hc$, where $\sigma_{1,2}(\lambda)$ are the

1 and 2 e–h pair excitation cross-sections, respectively, of a QD for an excitation wavelength λ . Since both the on/off-times of the QD are much longer [20] than 200 ns, the time window of the TAC (the on-times are in the millisecond range even at the highest studied intensities), we can assume p_+ constant in (4) and determine the average time evolution of p_1 for these short times. Using $p_0 + p_1 + p_+ = 1$, the initial conditions of $p_0(0) = 1$, $p_1(0) = 0$ and $\tau_{\text{off}}^{-1} \ll W_1$, we obtain

$$p_1(\tau) = \frac{W_1(1 - p_+)}{(W_1 + W_2 + 1/T_1)} \times \{1 - \exp[-(W_1 + W_2 + 1/T_1)\tau]\}. \quad (5)$$

During the accumulation of the histogram, p_+ stochastically takes the value 1 or 0 depending if the QD is ionized (off periods) or not (on periods). Only the on periods ($p_+ = 0$) contribute to the coincidence histogram. The effect of the off periods is to reduce the effective integration time. Thus, we can use the exponential rising function of $p_1(\tau)$ from (5) to fit the histogram $C(\tau)$. The inverse rise time constant approaches T_1^{-1} at low intensities and increases linearly with the intensity: $T_1^{-1}(1 + (I/I_s))$, where the parameter I_s is defined as the fluorescence saturation intensity. Assuming that the two e–h pair excitation rate is negligible, we can approximate $I_s \approx (1/\sigma_1 T_1)(hc/\lambda)$. Thus, this model recovers the expected behavior of a simple two-level system at short times, where the on/off blinking effects are minimal.

In Fig. 2, we plot the histogram of QD lifetimes deduced from the coincidence histograms of 66 QDs at low excitation intensities. The measured lifetimes are distributed between 12 and 28 ns with a mean value around 20 ns. The width of the distribution is not explained by experimental uncertainty (< 2 ns) and can be attributed to the heterogeneity in the structure of the QDs. These lifetimes are qualitatively in agreement with those recently measured by Dahan et al. [16] with a standard time-correlated single-photon-counting (TCSPC) method. While a multi-exponential function was necessary to fit the fluorescence decays from the TCSPC method, our data did not require more than a single exponential fit. One possible explanation given for the multi-exponen-

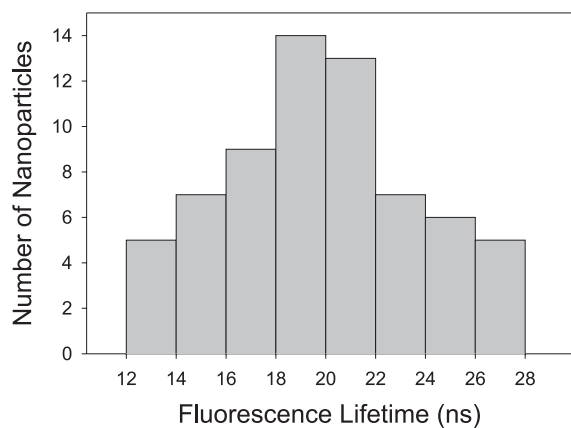


Fig. 2. Histogram of QD lifetimes measured from the coincidence histograms of 66 QDs at low excitation intensities. The measured lifetimes are distributed between 12 and 28 ns with a mean value around 20 ns.

tial behavior is the existence of a ‘dull’ state with a low radiative rate. This explanation implies that

our coincidence histograms should show a single exponential rise because the coincidence data are built primarily from the ‘bright’ state. The contribution of a dull state to $C(\tau)$ should be negligible since the probability of a coincidence event is proportional to the square of the dull state count rate which does not exceed 10 kHz for the highest studied intensities. Improving the signal to noise of our histogram may permit a multi-exponential fit and allow better comparisons with the lifetime measurements.

An example of the intensity dependence of the rise rates of $C(\tau)$ measured from the same single QD at different excitation intensities is shown in Fig. 3. The insets show the coincidence histograms measured at the lowest intensity (left) and the highest intensity (right). The linear fit of this dependence gives a fluorescence lifetime of $22 (\pm 1)$ ns and a fluorescence saturation intensity of $40 (\pm 3)$ kW/cm² for this QD. Using the expression for I_s , we deduce an absorption cross-section

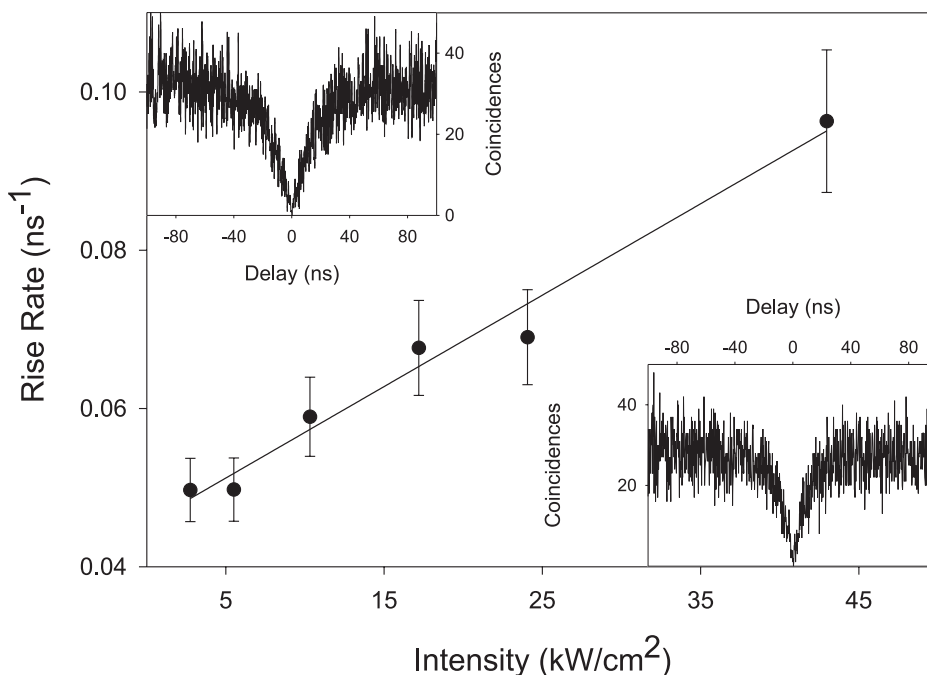


Fig. 3. Intensity dependence of the rise rates deduced from single exponential fits of the coincidence histograms measured from the same single QD at different excitation intensities. The linear fit gives a rate of $0.045 (\pm 0.002)$ ns⁻¹ at zero intensity, which corresponds to a fluorescence lifetime of $22 (\pm 1)$ ns, and a saturation intensity of $40 (\pm 3)$ kW/cm² for the QD. The insets show the coincidence histograms measured at the lowest intensity (left) and the highest intensity (right).

of $4.6 (\pm 0.4) \times 10^{-16} \text{ cm}^2$ at 488 nm for this QD. For the studied QDs (~ 13), we found fluorescence saturation intensities of 10–80 kW/cm^2 and absorption cross-sections of $2\text{--}16 \times 10^{-16} \text{ cm}^2$. As with the lifetime distribution above, these distributions of measured values may also be influenced by the structure of each QD and the exact position and orientation of the QD with respect to the laser beam. The cross-section values are consistent with the ensemble value $4 \times 10^{-16} \text{ cm}^2$ deduced from an approximate measurement of the extinction coefficient of a solution of QDs at 488 nm ($\epsilon \approx 10^5 \text{ cm}^{-1} \text{ M}^{-1}$).

To study the fluorescence saturation intensity in an independent manner, one would like to measure the average count rate of an individual QD at different excitation intensities. Usually this average count rate is obtained by integrating the emitted fluorescence over relatively long times (longer than 10 ms). For QDs, however, this method is only valid at low excitation intensity. At high intensity, the on-times of QDs decrease (to the millisecond range), causing the average count rate to be skewed. To remedy this, we use the coincidence histograms directly to obtain an accurate value for the average count rate in the on-state, since the background levels in our measurements are negligible. For a large TAC window and a high count rate, we cannot assume that the delay times τ are shorter than the mean time between detection events. Consequently $J(\tau)$ is no longer equivalent to $K(\tau)$. Instead, the probability densities $J(\tau)$ and $K(\tau)$ are related to each other by $\tilde{K} = \tilde{J}/(1 + \tilde{J})$ where \tilde{J} and \tilde{K} represent the Laplace transforms of $J(\tau)$ and $K(\tau)$. Using the expression for $J(\tau)$ and $p_1(\tau)$ from (3) and (5), it is straightforward to show that the coincidence histogram is given by

$$C(\tau) = G^{(2)}(\tau) \exp\left(-\eta_2 \Phi_f p_1^{\text{st}} \frac{\tau}{T_1}\right), \quad (6)$$

where p_1^{st} is the steady-state value of $p_1(\tau)$ during the on periods ($p_+ = 0$ and $\tau \gg T_1$ in (5)). Note that the quantity we seek, $R_2 = \eta_2 \Phi_f p_1^{\text{st}}/T_1$, is the average count rate of the stop detector (during an on period). Fig. 4 shows a histogram of delay times measured within an 8 μs TAC time window, the exponential decay implied by (6) is clearly

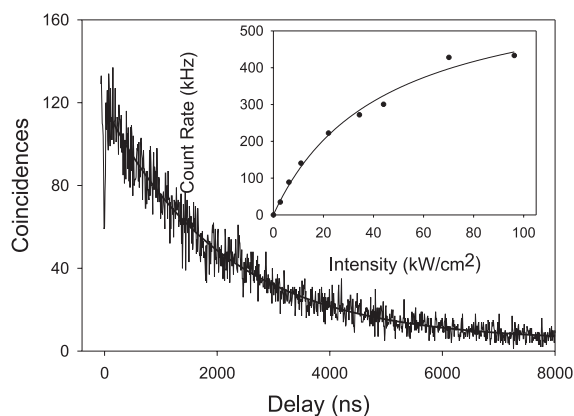


Fig. 4. Histogram of time delays between consecutive photon pairs over a time range of 8 μs at an intensity of 85 kW/cm^2 . The dip at $\tau = 0$ does not go to zero because of the histogram resolution. From the exponential decay of the signal, we deduce the average count rate of the stop detector. The inset shows a saturation intensity study using this method to determine the average count rate for intensities above 10 kW/cm^2 . The saturation intensity for this QD is 43 (± 7) kW/cm^2 .

evident. The antibunching dip at zero time delay does not reach zero because of the histogram resolution.

The inset of Fig. 4 shows a saturation study of the count rate of a single QD. For low excitation intensities, where the exponential decays are difficult to fit, the standard integration method is used. At high intensities, however, R_2 is deduced from the histogram decays. Using the expression for p_1^{st} as a fitting function, we obtain a total (from both detectors) saturation count rate of ~ 1 MHz. Assuming a total detection efficiency of $\sim 6\%$, we can estimate the fluorescence yield of the QD to be 40%, in reasonable agreement with the ensemble measured value. Furthermore, the saturation intensity obtained with this method (see Fig. 4) is comparable to that obtained from the rise rates of the coincidence histogram near $\tau = 0$ (see Fig. 3).

In this Letter, the second-order correlation behavior of photons emitted from a single QD has been described. Despite the possibility of multiple e–h pair creation, the fluorescence from single QDs shows strong photon antibunching over a wide range of intensities presumably due to the Auger ionization process which quenches any

multi-exciton state. By analyzing the data in a novel way, the fluorescence saturation intensity of the on-state has been determined to be within a factor of 2–5 of that for laser dye molecules, and the absorption cross-section has been determined in a fashion that does not rely on bulk concentration measurements. These results have particular relevance to the use of QDs as sources for quantum communication and cryptography. While the QD emission nicely mimics that from an isolated two-level system during the on-state periods, the presence of off-states with power law distribution over a broad time range [10] limits the applicability. Future materials development or secondary irradiation may be able to shorten the lifetime of the ionized (off) state.

Acknowledgements

B.L. acknowledges NATO for fellowship support. H.B. is a NSF Graduate Fellow. D.G. acknowledges a fellowship provided by the Swiss National Science Foundation. This work was partially supported by the National Science Foundation under Grant No. MCB-9816947 and by the Director, Office of Energy Research, Office of Basic Energy Sciences, Materials Sciences Division of the US Department of Energy under Contract No. DE-AC-76SF00098.

References

- [1] V.L. Colvin, M.C. Schlamp, A.P. Alivisatos, *Nature* 370 (1994) 354.
- [2] B.O. Dabbousi, M.G. Bawendi, O. Onitsuka et al., *Appl. Phys. Lett.* 66 (1995) 1316.
- [3] M.C. Schlamp, X. Peng, A.P. Alivisatos, *J. Appl. Phys.* 82 (1997) 5837.
- [4] M.J. Bruchez, M. Moronne, P. Gin et al., *Science* 281 (1998) 2013.
- [5] W.C.W. Chan, S. Nie, *Science* 281 (1998).
- [6] W.E. Moerner, M. Orrit, *Science* 283 (1999) 1670.
- [7] S.A. Empedocles, M.G. Bawendi, *Science* 278 (1997) 2114.
- [8] S.A. Empedocles, D.J. Norris, M.G. Bawendi, *Phys. Rev. Lett.* 77 (1996) 3873.
- [9] M. Nirmal, B.O. Dabbousi, M.G. Bawendi et al., *Nature* 383 (1996) 802.
- [10] M. Kuno, D.P. Fromm, H.F. Hamann et al., *J. Chem. Phys.* 112 (2000) 3117.
- [11] P. Roussignol, D. Ricard, J. Lukasik et al., *J. Optical Soc. Am. B* 4 (1987) 5.
- [12] H.J. Kimble, M. Dagenais, L. Mandel, *Phys. Rev. Lett.* 39 (1977) 691.
- [13] T. Basché, W.E. Moerner, M. Orrit et al., *Phys. Rev. Lett.* 69 (1992) 1516.
- [14] L. Fleury, J.-M. Segura, G. Zumofen et al., *Phys. Rev. Lett.* 84 (2000) 1148.
- [15] V.I. Klimov, A.A. Mikhailovsky, D.W. McBranch et al., *Science* 287 (2000) 1011.
- [16] M. Dahan, T. Laurence, F. Pinaud et al., in press, 2000.
- [17] O. Benson, C. Santori, M. Pelton et al., *Phys. Rev. Lett.* 84 (2000) 2513.
- [18] S. Reynaud, *Annales de Physique* 8 (1983) 315.
- [19] A.L. Efros, M. Rosen, *Phys. Rev. Lett.* 78 (1997) 1110.
- [20] U. Banin, M. Bruchez, A.P. Alivisatos, *J. Chem. Phys.* 110 (1999) 1195.